2019

The Role of Threonyl-tRNA Synthetase in Regulating Autophagy in Ovarian Cancer

Keira L. Goodell
University of Vermont

The Role of Threonyl-tRNA Synthetase in Regulating Autophagy in Ovarian Cancer

Keira Goodell, Biological Science B.S.

Alicia Ebert, Ph.D.
Karen Lounsbury, Ph.D.

Honors College Thesis

University of Vermont College of Arts & Sciences
Department of Biology

April 30, 2019

Abstract

Autophagy is the process by which lysosomes degrade and recycle damaged proteins and organelles in order to promote cell survival under situations of nutrient deprivation and homeostatic stress. Studies in the Lounsbury Lab have identified threonyl-tRNA synthetase (TARS) as a potential regulator in the autophagy pathway. *This study tests the hypotheses that TARS independently inhibits the process of autophagy within human ovarian cancer cells and that blocking TARS signaling increases markers of autophagy within tumors in a mouse model of ovarian cancer.* Ovarian cancer cells were cultured and transfected with siRNA to reduce TARS levels and quantitative Western blotting was employed to test the effects of TARS knockdown during amino acid starvation or mTOR inhibition. Changes were detected using antibodies against TARS, the positive autophagy markers p-AMPK and p-ULK, and the protein p62. TARS knockdown by siRNA was successful ($p<0.0001$) and TARS inhibition resulted in increased levels of p-AMPK ($p=0.0007$) and p-ULK ($p=0.003$). To assess *in vivo* effects of TARS activity on autophagy, mice were injected subcutaneously with ID-8 ovarian cancer cells. After three weeks, the animals were treated three times per week with either vehicle control or the TARS inhibitor BC194. Tumor sections were analyzed by immunohistochemistry to detect TARS, autophagy, and inflammatory markers. Tumors treated with BC194 were larger and showed increased levels of TARS. The results of this study have strong implications for the potential to identify a novel therapeutic target in ovarian cancer treatment.

Introduction

Aminoacyl-tRNA synthetases

The canonical function of aminoacyl-tRNA synthetases (ARSs) is in protein translation, where the enzymes catalyze the attachment of individual amino acids to their corresponding tRNAs (Park, Ewalt, & Kim, 2005). Once the tRNA has been "charged" with its appropriate amino acid according to the genetic code, the amino acid can be added to the growing protein peptide. The presence of ATP is required for the ARS to recognize the proper amino acid and perform the aminoacylation (**Figure 1**). As a consequence of their function, ARS enzymes are able to sense both the presence of energy in the form of ATP as well as the availability of amino acids within the cell. Previously thought of as only a "housekeeping enzyme," ARS enzymes have recently been found to play a role in a variety of other cellular functions.

Threonyl-tRNA synthetase (TARS) catalyzes the attachment of threonine to its cognate tRNA. Previous studies in the Lounsbury lab have concluded that TARS exerts angiogenic activity and stimulates endothelial cell migration in both *in vivo* and *in vitro* models using human umbilical vein endothelial cells (Williams, Mirando, Wilkinson, Francklyn, & Lounsbury, 2013). Both angiogenic and metastatic capabilities contribute to the malignancy and poor prognosis associated with human ovarian cancer. This conclusion led to further studies investigating the role of TARS in ovarian cancer tumor progression. Data from the Lounsbury lab offered the first positive correlation between increasing disease stage and TARS expression in human ovarian cancer cells (Wellman et al., 2014). Though overexpression of TARS was correlated with increased cancer aggression, Cox proportional hazard models showed that TARS expression within the tumor was inversely correlated with mortality in late stage disease (Wellman et al., 2014). The mechanism by which TARS is interacting with the cancer cells to create these effects

is still largely unknown, though autophagy-mediated changes in the tumor microenvironment have been observed in ovarian and breast cancer models (Mowers, Sharifi, & Macleod, 2017).

The current research interest of the Lounsbury lab is the role of TARS in autophagy. *The goal of this study was to test the hypotheses that TARS independently inhibits the process of autophagy within human ovarian cancer cells and that blocking TARS signaling increases markers of autophagy within tumors in a mouse model of ovarian cancer*.

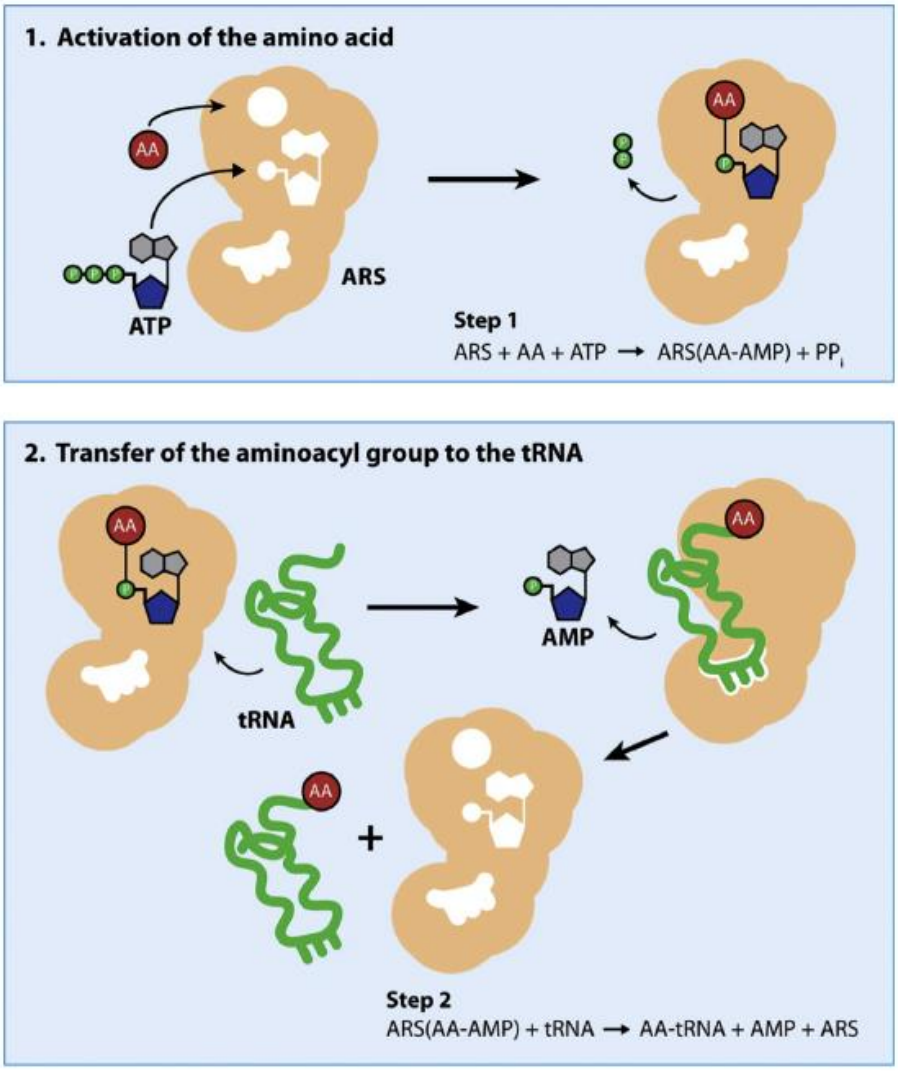

Figure 1: Canonical Function of Aminoacyl-tRNA Synthetase. Aminoacyl-tRNA synthetases (ARSs) play an integral role in the conversion from genetic code to functional protein. ARSs are ATP-dependent enzymes which catalyze the attachment of amino acids to the proper tRNA. The amino acid is then added to the growing protein peptide (from Rajendran et al., 2018).

Autophagy Signaling

Autophagy is the process by which cells selectively digest and recycle internal organelles and structures. Autophagy is activated in response to low nutrient availability and other forms of stress such as oxygen deprivation, with the products of autophagy-mediated degradation including the building blocks of protein synthesis (Behrends, Sowa, Gygi, & Harper, 2010). Autophagy is a complex system regulated by a network of over 30 autophagy-related gene (ATG) proteins (Xu et al., 2019). There are several types of autophagy that are known and understood. Microautophagy is the process by which lysosomes engulf cytoplasmic materials via invagination of the lysosomal membrane. Chaperone-mediated autophagy is achieved by chaperones, co-chaperones, and a lysosomal-associated membrane protein. Macroautophagy, the focal point of this paper which will hereby be referred to as "autophagy," is characterized by the formation of a double-membrane organelle called an autophagosome (Jiang & Mizushima, 2014). Formation of the autophagosome is the rate-limiting step in the initiation of autophagy and requires more than 20 different autophagy-related proteins (Meijer & Codogno, 2008). Autophagosomes collect both stable and unstable cellular contents and then fuse with lysosomes, forming autophagolysosomes (**Figure 2**). It is within these autophagolysosomes that degradation and recycling occurs (White, Mehnert, & Chan, 2015).

Autophagy is a sort of double-edged sword within human cell lines. When a tumor is initially emerging, autophagy has a preventative effect against development and growth of the cancer. Cells utilize lysosomal degradation to prevent the accumulation of damaged organelles and the proliferation of mutated DNA. Thus, early in cancer development, autophagy works in conjunction with DNA repair as a sort of gatekeeping mechanism to ensure that everything is in order. However, once a tumor has developed and established itself within the tissue, the cancer cells exploit autophagy for their own protection (Jiang & Mizushima, 2014). During scenarios of

extreme nutrient deprivation and oxidative stress—such as radiation and chemotherapy—the cancer cells are almost entirely reliant on autophagy-mediated recycling to sustain baseline function (Kung, Bergenstock, Balaburski, Budina, & Murphy, 2012). Upregulation of autophagy allows cancer cells to survive under conditions which would otherwise result in their degradation, thereby promoting cancer survival and proliferation.

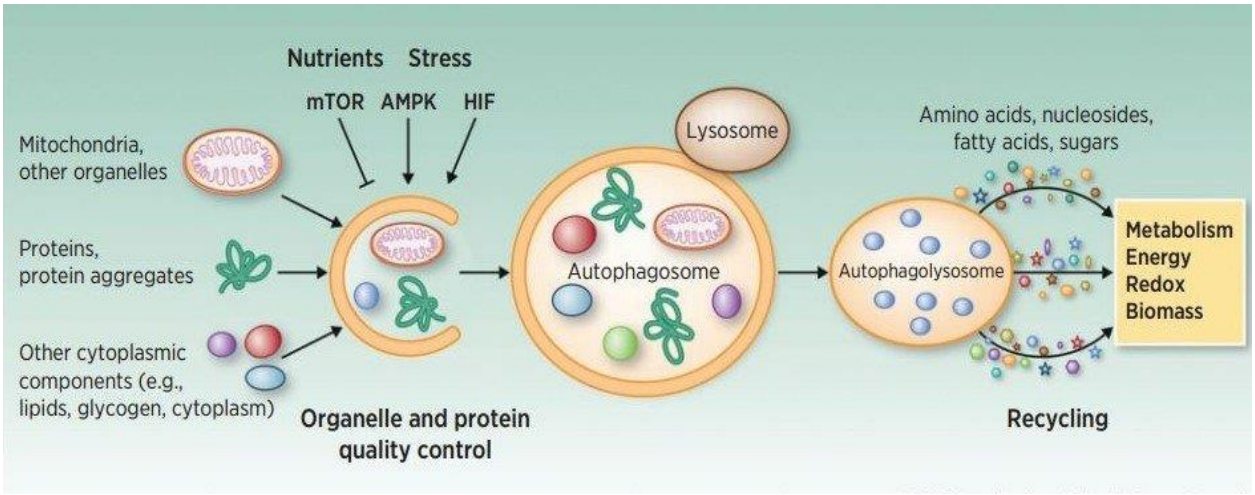

Figure 2: Process of Macroautophagy. Nutrient deprivation and stress result in damaged organelles, proteins, and cytoplasmic components being engulfed in a double membrane autophagosome. The autophagosome then fuses with a lysosome to form an autophagolysosome, where these components are degraded and recycled to be used for metabolism and energy (from White et al., 2015).

Nutrient deprivation is the most well understood inducer of autophagy through a pathway that includes AMP-activated protein kinase (AMPK) and UNC-51 like activating autophagy kinase (ULK1). AMPK is an enzyme with the ability to sense the AMP:ATP ratio within the cell and thus monitor energy availability (Kung et al., 2012). When the cell is deprived of nutrients and energy stores are low, AMPK is activated via phosphorylation. Phospho-AMPK (p-APMK) induces autophagy indirectly via inhibition of mechanistic target of rapamycin (mTOR). mTOR is a known and established inhibitor of autophagy which is activated only in the presence of amino acids, ensuring that autophagy is inhibited only if the cell has ample materials available

for metabolism (Meijer, Lorin, Blommaart, & Codogno, 2015). p-AMPK can also induce autophagy directly via phosphorylation of ULK1.

The ULK1 complex contains the protein kinases ULK1/2 and is essential for the formation of the autophagosome and the induction of autophagy (Meijer et al., 2015). p-AMPK and mTOR both phosphorylate the ULK1 complex with antagonistic effects on autophagy induction. While ULK1 phosphorylation by p-AMPK induces autophagy via formation of the autophagosome, ULK1 phosphorylation by mTOR occurs at a different site and inhibits autophagy via dissociation and inactivation of the ULK1 complex (Meijer et al., 2015).

The ubiquitin- and LC3-binding protein p62 is commonly used as an autophagy-related marker (Xu et al., 2019). p62 plays a critical role in the formation of intracellular protein aggregates which are subsequently engulfed by the autophagosome (Komatsu et al., 2007). p62 itself is engulfed and degraded during the autophagic process after forming a complex with ubiquitinated proteins and LC3 (Xu et al., 2019). Inhibition of autophagy has been associated with accumulation of p62 within the cytoplasm (Xu et al., 2019).

The proposed hypothesis predicts a role for TARS-mediated autophagy inhibition that is independent of mTOR (**Figure 3**). The positive autophagy markers p-AMPK and p-ULK are used as a proxy to quantify the induction/inhibition of autophagy within the cultured cell lines.

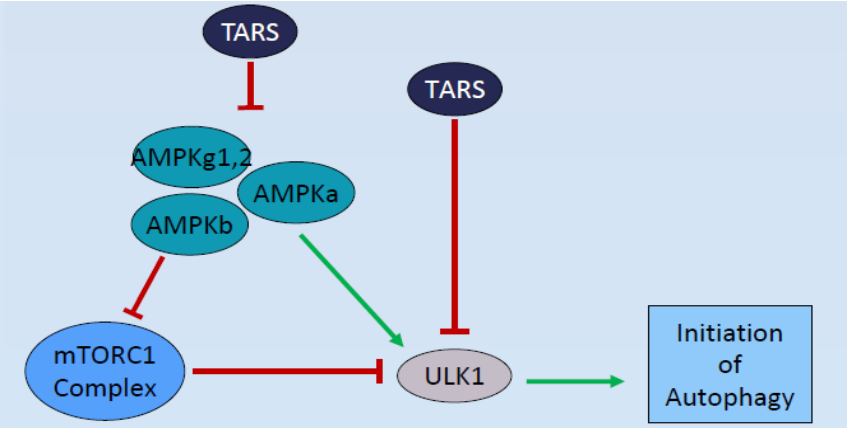

Figure 3: Proposed Autophagy Pathway. mTOR inhibits autophagy via phosphorylation and dissociation of ULK1. AMPK initiates autophagy via phosphorylation and activation of ULK1. It is proposed that TARS inhibits autophagy independently of mTOR via AMPK and ULK1 inhibition (from Andrews et al, 2018).

Autophagy and Ovarian Cancer

Because of the complicated interaction of pathways involved in autophagy signaling, dysregulation of these pathways has been implicated in the etiologies of several human diseases including type 2 diabetes, heart and liver disease, lysosomal storage disorders, and cancer (Meijer et al., 2015). The American Cancer Society reported in 2009 that ovarian carcinoma was the gynecologic malignancy with the highest case-to-fatality ratio, with 69% of all diagnosed patients dying of the disease (Lengyel, 2010). Epithelial ovarian cancer owes its high mortality rate to several factors. There is a lack of effective testing to detect early stage disease, especially in pre-menopausal women, resulting in late stage diagnosis for most patients (Wellman et al., 2014). Coupled with this late stage diagnosis is a vast majority of patients presenting with already widely metastatic disease (Lengyel, 2010). Finally, mortality is associated with a high instance of tumor relapse following anticancer therapies. Tumor progression and relapse have largely been contributed to cancer stem cells which retain the ability to survive nutrient starvation and treatment with chemotherapy (Pagotto et al., 2017). This resistance to chemotherapy has been associated with autophagy activation within malignant cells.

Studies suggest a role for autophagy in several steps of the metastatic cascade. The metastatic cascade is the process by which a cancer physically leaves the primary site to establish and grow at a secondary site. The cascade occurs in stages: local invasion at a primary site, intravasation to the blood or lymphatic system, survival in circulation, extravasation to the secondary site, and survival and growth at the secondary site (Mowers et al., 2017). Movement in every stage of the metastatic cascade subjects the cancer to cellular stressors such as nutrient deprivation, hypoxia, and lack of physical support. Increased autophagy has been observed in cancer stem cells, assisting the epithelial-mesenchymal transition and allowing the cancer to survive in a changing microenvironment (Mowers et al., 2017). Autophagy has also been found

to play a key role in modulating tumor dormancy and drug resistance (Mowers et al., 2017). It is possible that combining autophagy inhibition with classical anticancer therapies will target the epithelial ovarian cancer stem cell population, overcoming the current treatment limits (Pagotto et al., 2017). Additional information about the cellular mechanisms and regulation of autophagy must be obtained before assessing the validity of any such therapy options.

TARS and Autophagy

The proposed involvement of TARS in the autophagy pathway is the basis for this study. Previous studies have shown that knockdown of genes encoding ARS enzymes rescued animals from hypoxia-induced death (Anderson, Mao, Scott, & Crowder, 2009). This suggests that decreasing ARS expression allows cells to better perform the autophagic processes required for survival. Studies in the Lounsbury lab have concluded that TARS, but not seryl- or tyrosyl-tRNA synthetase, is overexpressed in ovarian cancer cells (Wellman et al., 2014). We predicted that TARS inhibits autophagy independently of mTOR via direct interaction with the ULK1 complex and AMPK. This prediction was tested by reducing TARS levels using siRNA knockdown in cultured ovarian cancer cells and by examining ovarian tumor sections from mice that had been treated with a TARS inhibitor. In both systems, antibodies were utilized to quantify the amount of p-ULK and p-AMPK present in cell lysates or tissue sections. This quantification was then used as a proxy to determine the levels of autophagy occurring within the cell under normal conditions and in the absence of TARS.

This study hopes to elucidate the functions of autophagy in tumor cells so that autophagy inhibitors may be used in the clinical setting to treat or prevent the spread of metastatic cancer. ARS enzymes have already been identified as potential drug targets for a variety of human maladies (Rajendran, Kalita, Shukla, Kumar, & Tripathi, 2018). Due to the structural similarity

of ARS enzymes in different organisms, the potential for testing the effects of ARS inhibition is promising in non-human models. Potential targets of autophagy induction or inhibition have been identified in many different disease states (Galluzzi, Pedro, Levine, Green, & Kroemer, 2017) (**Figure 4**). Understanding the role of TARS in cancer cell autophagy will contribute to the greater understanding of using ARS enzymes as pharmaceutical targets in the treatment of cancer and other illnesses.

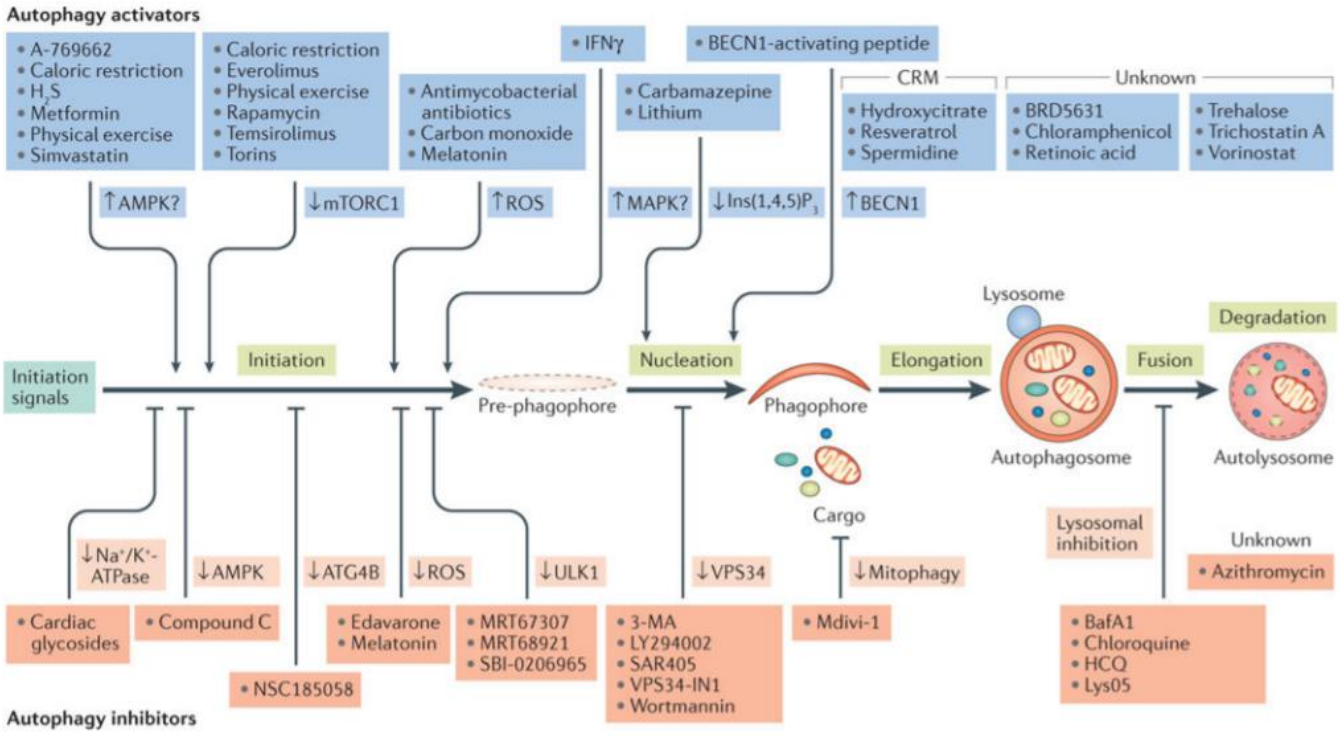

Figure 4: Interaction of known autophagy activators and inhibitors with the autophagy induction sequence. Current pharmacological interventions to inhibit or enhance autophagy at the initiation, nucleation, elongation, fusion, or degradation phases (from Galluzzi et al., 2017).

Methods

To test the hypothesis that TARS independently inhibits the process of autophagy within human ovarian cancer cells, quantitative Western blotting using primary antibodies against autophagy markers was employed.

Western Blotting

SKOV3 cells: The cells used in this experiment were SKOV3 human ovarian cancer cells. These cells were cultured in McCoys media + 10% fetal bovine serum and passaged using trypsin to generate 1 10 cm plate/condition. Cells were grown in an incubator at 37◦C with 5% CO_2.

Cell Transfection: Cells were transfected one day after passage. For siRNA, cells were exposed to TARS siRNA (siTARS) or non-targeting control siRNA (siControl) using the siTRAN™ protocol. Cells were incubated for 4-6 hours and then the media was changed to antibiotic-free McCoys. Cells were then harvested approximately 48 hours after transfection.

Cell Treatments: One day after transfection, the cells were treated with either DMSO (vehicle control), amino acid starvation media (EBSS), or Torin1 (mTOR inhibitor). Each of the experimental treatments were performed for siControl and siTARS so that the results of the treatments could be confidently attributed to the treatments themselves.

Protein Extracts: Following treatments (16 hr), cells were harvested to make protein extracts using the protocol by Williams et al. (Williams et al., 2013). Briefly, the plates were washed with phosphate buffered saline and modified RIPA buffer was added to each plate. The contents of the plates were then scraped and transferred into a correspondingly labeled microfuge tube and frozen at -80◦C. To ensure equal protein loading, 2 μl from each sample was used to determine protein concentration using the Bradford protein assay.

SDS-PAGE and Western Blot: Protein samples (10 µg) were boiled in Laemmli sample buffer and separated by 8% SDS-PAGE. Molecular weights of bands were determined using a pre-stained molecular weight marker. Proteins were transferred to nitrocellulose (blot) and blocked in 3% milk in Tris-buffered saline/tween-20 (TBST). The blots were exposed overnight to primary antibodies diluted 1:1000 in 3% BSA/TBST + 0.1% azide. Primary antibodies supplied by GeneTex and Cell Signaling Technology included: GTX116359 Rab anti-TARS, CS21285 Rab anti-β-tub, CST2535 Rab anti-p-AMPK, CST6888 Rab anti-p-ULK1 (3757), and CST5114 Rab anti-SQSTM1/p62. After incubation, the primary antibody was recovered, and the blots were washed several times with TBST. Secondary antibody (HRP-Goat-anti-rabbit IgG, Jackson Laboratories) was applied at a dilution of 1:5000 in 3% BSA/TBST. After thorough washing with TBST, blots were developed using chemiluminescence (Clarity™) (**Figure 5**). Imaging and quantification of blots were performed using the Biorad AI600.

Statistical Analysis: Western blot band pixel intensities were determined using the software on the Biorad AI600 using rolling ball background subtraction. Statistical analysis of the results was generated by Graphpad/Prism using 2-way ANOVA for multiple comparisons.

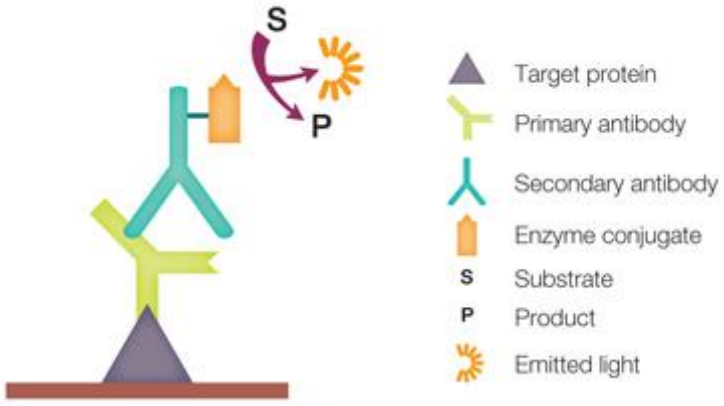

Figure 5: Interaction of primary and secondary antibodies with Clarity™ chemiluminescence. The primary antibody specific to a single target protein binds to the protein on the gel. Species-specific secondary antibody recognizes and binds to the primary antibody. The horse radish peroxidase enzyme activity conjugated to the secondary antibody converts the applied chemiluminescence substrate into product and emitted light, which is detected by the Bio-Rad AI600 (from Bio-Rad Clarity™ and Clarity Max™ Western ECL Blotting Substrates).

To test the hypothesis that blocking TARS signaling increases markers of autophagy within tumors in a mouse model of ovarian cancer, immunohistochemistry using primary antibodies against autophagy markers was employed.

Immunohistochemistry

Source of Ovarian Tumor Sections: Note, no animals were used specifically for this study, only tumor sections from a previous study. To generate tumor sections for this study, female mice were anesthetized and subcutaneously injected in the flank with ID8 mouse ovarian cancer cells. Three weeks following initial injection, animals were injected intraperitoneally with either vehicle control or TARS inhibitor BC194 (2 mg/kg) three times per week for four weeks. Tumors were resected and embedded in paraffin (**Figure 6**). Tumor sections (10 μm) were transferred to slides for antibody staining.

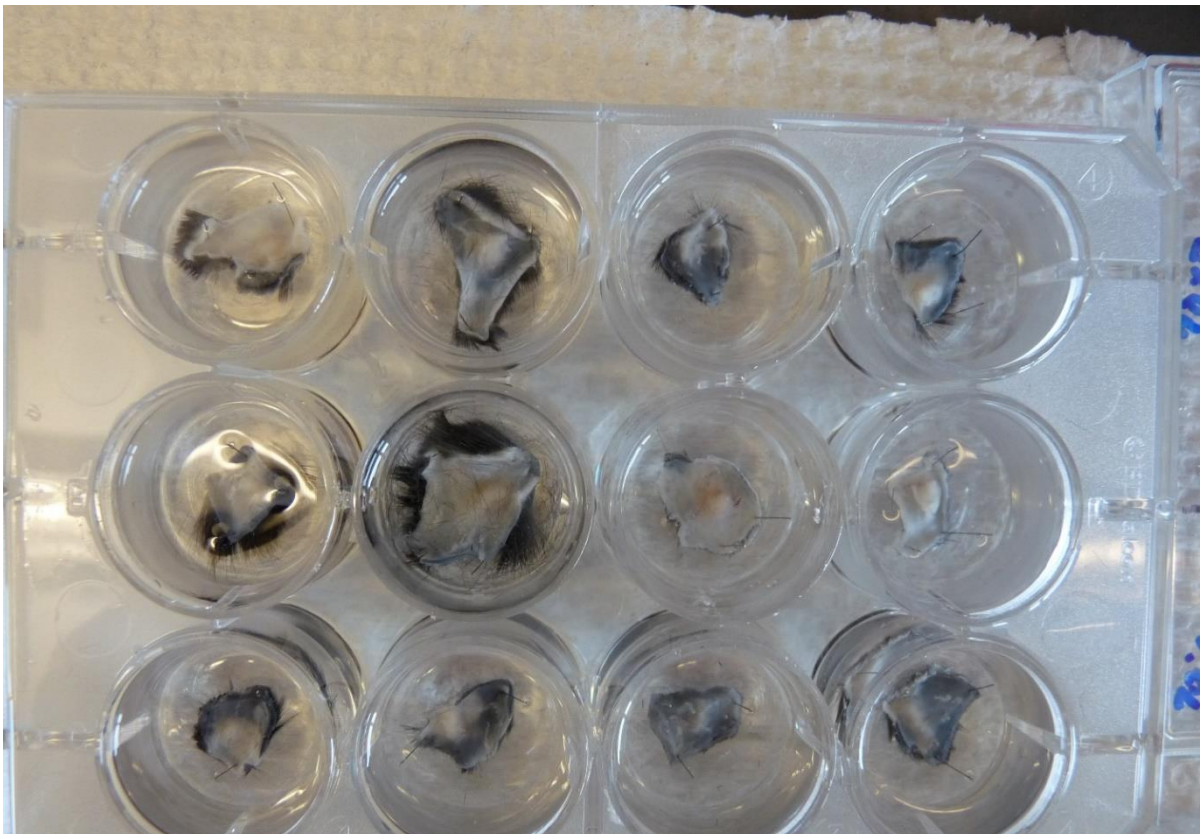

Figure 6: Resected flank ID8 ovarian cancer tumors treated with vehicle control or BC194. Female mice were injected in the bilateral flanks with an equal number of ID8 ovarian cancer cells. After treatments 3x per week for 4 weeks, mice were sacrificed and tumors were resected for fixation.

Antibody staining of sections: The slides were dewaxed and rehydrated using xylenes followed by decreasing concentrations of ethanol. After rinsing in water, the samples were unmasked in plastic Coplin jars using DAKO Antigen Retrieval solution at 98℃ for 20 minutes and subsequently allowed to cool at room temperature for 20 minutes. The slides were washed three times with deionized water. Endogenous peroxide activity was quenched with peroxidase block (4ml 30% H_2O_2 + 36ml methanol per Coplin jar) for 10 minutes. The slides were washed once with deionized water and then for 5 minutes in PBS. All slides were blocked with two drops of Vector Normal Horse serum, except the F4/80 for which Normal Goat serum was used. The slides were left at room temperature for one hour under parafilm. Excess solution was drained from the slides.

Antibodies: Primary antibodies were: GTX116359 Rab anti-ThrRS (TARS) (1:200), Cell signaling rab anti-P-ULK1 (S555) (1:200), Cell signaling rab anti-P-AMPK (1:200), and AbD MCA497GA Rat anti-F4/80 (1:250) in 3% BSA /0.2% TX-100/ PBS. Antibodies were applied to the sections, they were covered with parafilm, and then they were incubated for 24 hours in a humidity box at 4℃. After incubation, slides were washed with PBS 3 x 5 minutes while rocking. Excess solution was blotted off. Secondary antibodies were applied (2 drops) using Vector Labs # MP-7401 ImmPRESS Polymer HRP horse anti-rabbit IgG or goat anti-rat IgG for F4/80. Slides were incubated for one hour at room temperature in the dark.

Developing: Slides were developed with ImmPACT developer (36 µl DAB (diaminobenzidine)/ml diluent) 10 min and then counterstained with filtered Mayer's hematoxylin for one minute. Slides were dehydrated through increasing concentrations of ethanol followed by xylenes and mounted with Cytoseal-60. Images were collected on an Olympus BX50 Light Microscope in the Microscopy Imaging Center.

Results

To determine whether reducing TARS levels results in the induction of autophagy, SKOV3 cells were incubated with either non-targeting control siRNA (siCon) or TARS-specific siRNA (siTARS). Cells were then treated with either the mTOR inhibitor Torinn1 or with starvation media (EBSS) to stimulate autophagy. Western blot of the cell lysates was performed to detect TARS, p-AMPK, p-ULK1, p62, and β-tubulin.

Bands shown in Figure 7a show the predicted molecular mass of TARS is 83 kDa, the predicted molecular mas of p-ULK phosphorylated at the Serine 757 site is 140-150 kDa, the predicted molecular mass of p-AMPK phosphorylated at the Threonine 173 site is 62 kDa, and the predicted size of p62 is 62 kDa (**Figure 7A**). Protein loading was determined by levels of β-tubulin at 50 kDa and quantification was normalized to the intensity of the β-tubulin band.

Western blot quantification of TARS shows successful knockdown of TARS by siRNA ($p<0.0001$), with an average knockdown of 80% (**Figure 7B**). Successful siRNA knockdown allows the results to be attributed to reduced TARS levels alone without needing to account for the effect of treatment with siRNA. In the control treatment, TARS knockdown by siRNA resulted in increased levels of p-ULK ($p=0.003$) and p-AMPK ($p=0.0007$) compared to siControl (**Figure 7B**). This suggests that TARS inhibition induces autophagy. In the Torin1 treatment, levels of p-ULK were slightly elevated in the siTARS group compared to siControl, though this result was not significant ($p=0.07$) (**Figure 7B**). There was no effect of siTARS on levels of p-AMPK or p62 in the Torin1 treatment. Within the siControl group, there was a significant increase in p-ULK ($p=0.03$) and p-AMPK ($p=0.0095$) in the EBSS treatment when compared to the control treatment (**Figure 7B**), confirming that amino acid starvation induces autophagy in healthy cells. There was no effect of siRNA transfection or treatment on levels of p62.

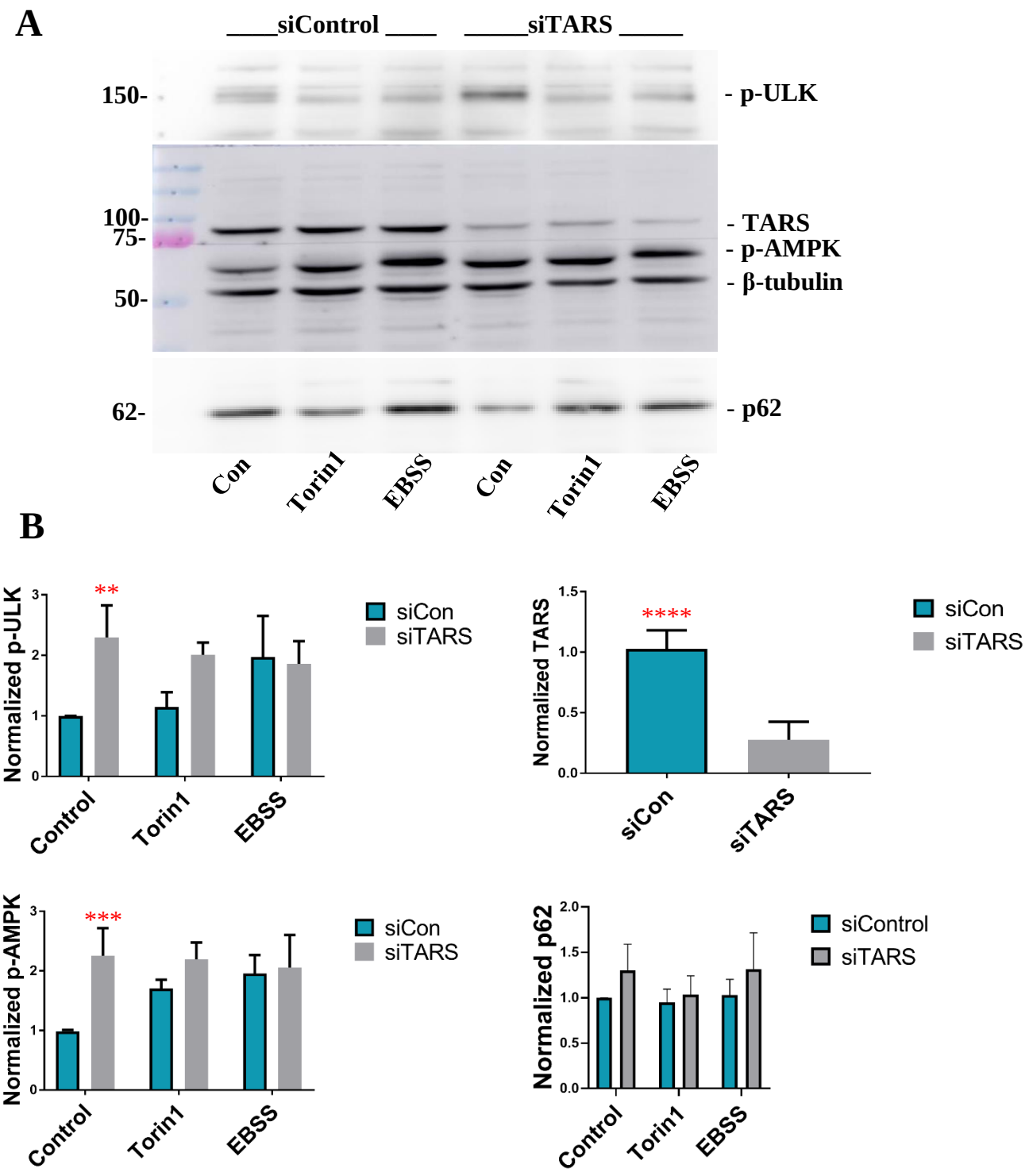

Figure 7: The effects of TARS knockdown on expression of p-ULK, TARS, p-AMPK, and p62 under control, Torin1, and EBSS treatments. A, Western blot of SKOV3 cells exposed to either non-targeting control siRNA (siCon) or TARS-specific siRNA (siTARS) treated with primary antibodies against p-ULK, TARS, p-AMPK, β-tubulin, and p62. Lanes 1, 4 are control treatment; lanes 2, 5 are Torin1 (mTOR inhibition) treatment; lanes 3, 6 are EBSS (amino acid starvation) treatment. β-tubulin used as loading control. B, Western blot quantifications normalized against loading control. Columns and error bars represent mean and standard deviation. ****p<0.0001; ***p=0.0007; **p=0.003. n=4.

To determine if loss of TARS also affects autophagy *in vivo*, the effects of the TARS inhibitor BC194 on the growth and autophagy of ovarian cancer flank tumors was measured. Mouse flank tumors treated with BC194 appeared larger in size than tumors treated with vehicle control (**Figure 8A**). This suggests that TARS enzyme inhibition allowed the cancer cells to propagate more effectively than cells with normal levels of TARS enzymatic activity. TARS staining increased with BC194 treatment compared to vehicle control (**Figure 8A**), representing a potential compensatory effect of enzyme inhibition. Both vehicle control and BC194 treatments showed macrophage invasion with F4/80 staining (**Figure 8A**). Tumors treated with BC194 had elevated levels of active site-phosphorylated ULK and AMPK compared to control (**Figure 8B**), suggesting an induction of autophagy, although these data were more variable.

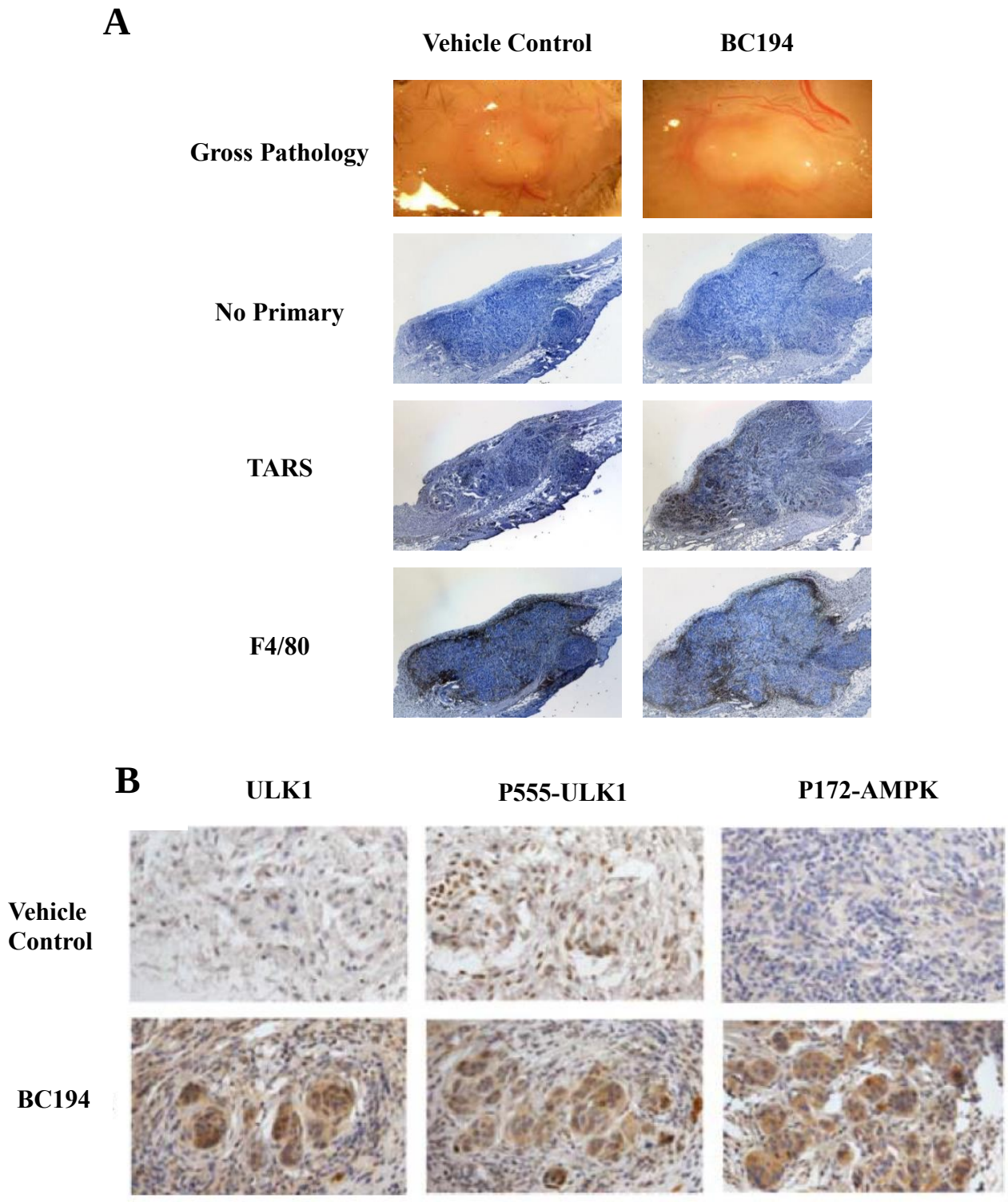

Figure 8: The effect of TARS enzyme inhibition on tumor pathology, expression of TARS, p-ULK, and p-AMPK, and macrophage infiltration. Tumors treated with vehicle control or TARS enzymatic activity inhibitor BC194. A, sections of tumor gross pathology, histology with no primary antibody, and immunohistochemistry staining using primary antibodies against TARS and F4/80, a mouse macrophage marker, n=8. B, antibody staining against ULK1 and the activating phospho-sites of ULK1 and AMPK, n=2.

Discussion

The overall goal of this study was to test the hypothesis that TARS is a negative regulator of autophagy, thus reducing TARS expression/activity would result in the induction of autophagy. Successful TARS knockdown of 80% using siRNA allowed the obtained results to be attributed to the individual treatments (**Figure 7B**). Increased levels of p-ULK and p-AMPK in the siTARS group compared to the siControl group suggest that TARS inhibition results in induction of autophagy (**Figure 7B**). The hypothesis that TARS inhibits autophagy is supported by these results. If p62 was involved in the TARS signaling pathway, it would be predicted that levels of p62 decrease with autophagy induction, as p62 is degraded in the autophagic process. Because there was no effect of TARS knockdown on levels of p62, it is possible that this degradation product may be a part of a separate, unrelated autophagy mechanism (**Figure 7B**). If TARS-mediated autophagic inhibition occurs independently of the mTOR complex, it would be predicted that levels of p-ULK and p-AMPK would be greater in the siTARS Torin1 treatment than in the siControl Torin1 treatment. Levels of p-ULK and p-AMPK appear to be slightly elevated in the siTARS treatment compared to siControl, but these results were not significant (**Figure 7B**). The hypothesis that TARS inhibits autophagy independently of mTOR was not supported by the data. Amino acid starvation should induce autophagy in healthy cells and thus was used as a positive control. EBSS treatment did result in significantly increased levels of p-ULK and p-AMPK in the siControl group compared to the control treatment (**Figure 7B**). There did not appear to be a combination effect of TARS inhibition and amino acid starvation, as there was no increase in positive autophagy markers between the control and EBSS treatments in the siTARS group (**Figure 7B**). This may be because TARS is acting as the sensor of energy availability within the cell and thus when TARS is inhibited the cell can no longer react as efficiently to low nutrient levels.

In the *in vivo* mouse tumor study, treatment with the Borrelidin derivative BC194 resulted in tumors that appeared larger in size and possibly had more extensive blood vessel growth (**Figure 8A**). These results were unexpected because previous work by the Lounsbury lab suggested that TARS promotes angiogenesis. It is possible that autophagy inhibition is the mechanism by which TARS produces these effects and that the increased size of tumors is primarily due to infiltrating macrophages. BC194 treatment resulted in increased levels of TARS staining in mouse tumor models of ovarian cancer (**Figure 8A**). This result may represent a compensation effect whereby TARS enzyme inhibition results in increased expression of TARS. Such a compensation effect has been documented in the use of phosphatidylinositol 3-kinase (PI3K) enzyme inhibitors in the treatment of non-small cell lung cancer. Response to inhibition of class IA PI3K enzymes suggested that PI3K isoforms may functionally compensate for one another to limit the efficacy of single agent treatments (Stamatkin, Ratermann, Overley, & Black, 2015). TARS inhibition did not dramatically effect tumor macrophage infiltration compared to vehicle control, although it was slightly elevated (**Figure 8A**). Tumor-associated macrophages are always abundant in malignant tumors. These macrophages promote angiogenesis, extravasation, and suppression of antitumor immune mechanisms (Yang, Mckay, Pollard, & Lewis, 2018). For these reasons, it would be predicted that more aggressive and larger tumors would show increased levels of macrophage staining. Qualifying the degree of antibody stain on a tumor section is very difficult and quite subjective. It is possible that there are different levels of staining between the control and BC194 tumors that cannot be detected. It is also possible that the tumors were not able to grow for long enough to see the changes in macrophage infiltration associated with increased aggressiveness and size. It is expected to see some autophagy in control tumors characterized by ULK1 and activated p-ULK1 and p-AMPK (**Figure 8B**). Tumors are often subjected to anoxic environments with low nutrient availability

and thus upregulate autophagy in order to sustain baseline function. Tumor treatment with BC194 resulted in noticeable increases in ULK1, p-ULK1, and p-AMPK staining (**Figure 8B**). This suggests that TARS enzyme activity works to prevent the initiation of autophagy and the formation of active, phosphorylated ULK1 and AMPK. The proposed mechanism suggests that TARS acts directly on AMPK to prevent activation of the ULK1 complex (**Figure 3**). The proposed mechanism also predicts that TARS acts directly on the ULK1 complex to promote its inactivation and dissociation (**Figure 3**). Increased levels of positive autophagy markers p-ULK and p-AMPK with BC194 treatment support the hypothesis that blocking TARS signaling increases markers of autophagy within tumors in a mouse model of ovarian cancer.

A future direction for this study is understanding the mechanism by which TARS interacts with autophagy proteins. The interaction of TARS with the positive autophagy protein ULK1 can be determined by subjecting purified ULK1 to an aminoacylation reaction with purified TARS. The products of the reaction can then be separated by SDS/PAGE and analyzed via mass spectroscopy to determine the mechanism of TARS/ULK1 interaction. Understanding this interaction will give insights into how ULK1 can be modified to alter the rate of autophagy within cancer cells. ULK1 is post-translationally acetylated and stimulated by the acetyltransferase TIP60 to induce autophagy (Narita, Weinert, & Choudhary, 2019). TARS may be catalyzing the threonylation and inactivation of ULK1 in order to inhibit autophagy. Further studies with the goal of identifying this potential new autophagy signaling mechanism are necessary in order to understand the greater significance of the observed results.

The results of this study as well as future studies investigating non-canonical functions of ARS enzymes have the capacity to elucidate a potential new target in chemotherapeutic intervention. Borrelidin analogues with decreased cytotoxicity have been biosynthetically engineered for the purpose of anti-angiogenic use in cancer therapy (Wilkinson et al., 2006).

Drugs targeting TARS also have the potential to be utilized as autophagy regulators, supplementing standard chemotherapeutic treatment regimens. Overall, this study used a combination of *in vitro* and *in vivo* experiments to show that TARS inhibits the process of autophagy within ovarian cancer cells. This project has led to a better understanding of where TARS fits into the autophagic process and has the potential to affect the future approach to treatment of ovarian cancer.

Acknowledgments

I would like to thank Dr. Karen Lounsbury for her incredible guidance throughout the experimentation, troubleshooting, and writing stages of this project. I would like to thank Theresa Wellman and Dr. Christopher Francklyn for their assistance with performing experiments and interpreting data. The UVM Office of Undergraduate Research provided funding for this project over Summer 2018. Additional funding was provided by the Francklyn Laboratory and the Department of Obstetrics and Gynecology through collaborations with Dr. Cheung Wong and Dr. Elizabeth McGee. Tumor images were obtained using the Olympus BX50 Light Microscope in the Microscopy Imaging Center.

References

Anderson, L. L., Mao, X., Scott, B. A., & Crowder, C. M. (2009). Survival from Hypoxia in. *Science*, *323*(January), 630–633.

Behrends, C., Sowa, M. E., Gygi, S. P., & Harper, J. W. (2010). Network organization of the human autophagy system. *Nature*, *466*(7302), 68–76.

Galluzzi, L., Pedro, J. M. B. S., Levine, B., Green, D. R., & Kroemer, G. (2017). Pharmacological modulation of autophagy: therapeutic potential and persisting obstacles. *Nature Reviews Drug Discovery*, *16*(7), 487–511.

Jiang, P., & Mizushima, N. (2014). Autophagy and human diseases. *Cell Research*, *24*(1), 69–79.

Komatsu, M., Waguri, S., Koike, M., Sou, Y. shin, Ueno, T., Hara, T., … Tanaka, K. (2007). Homeostatic Levels of p62 Control Cytoplasmic Inclusion Body Formation in Autophagy-Deficient Mice. *Cell*, *131*(6), 1149–1163.

Kung, C.-P., Bergenstock, M. K., Balaburski, G., Budina, A., & Murphy, M. (2012). Autophagy in tumor suppression and cancer therapy. *Critical Reviews™ in Eukaryotic Gene Expression*, *21*(1), 71–100.

Lengyel, E. (2010). Ovarian cancer development and metastasis. *American Journal of Pathology*, *177*(3), 1053–1064.

Meijer, A. J., & Codogno, P. (2008). Autophagy: A Sweet Process in Diabetes. *Cell Metabolism*, *8*(4), 275–276.

Meijer, A. J., Lorin, S., Blommaart, E. F., & Codogno, P. (2015). Regulation of autophagy by

amino acids and MTOR-dependent signal transduction. *Amino Acids*, *47*(10), 2037–2063.

Mowers, E. E., Sharifi, M. N., & Macleod, K. F. (2017). Autophagy in cancer metastasis. *Oncogene*, *36*(12), 1619–1630.

Narita, T., Weinert, B. T., & Choudhary, C. (2019). Functions and mechanisms of non-histone protein acetylation. *Nature Reviews Molecular Cell Biology*, *20*, 156–174.

Pagotto, A., Pilotto, G., Mazzoldi, E. L., Nicoletto, M. O., Frezzini, S., Pastò, A., & Amadori, A. (2017). Autophagy inhibition reduces chemoresistance and tumorigenic potential of human ovarian cancer stem cells. *Cell Death & Disease*, *8*(7), 1–10.

Park, S. G., Ewalt, K. L., & Kim, S. (2005). Functional expansion of aminoacyl-tRNA synthetases and their interacting factors: New perspectives on housekeepers. *Trends in Biochemical Sciences*, *30*(10), 569–574.

Rajendran, V., Kalita, P., Shukla, H., Kumar, A., & Tripathi, T. (2018). Aminoacyl-tRNA synthetases: Structure, function, and drug discovery. *International Journal of Biological Macromolecules*, *111*, 400–414.

Stamatkin, C., Ratermann, K. L., Overley, C. W., & Black, E. P. (2015). Inhibition of class IA PI3K enzymes in non-small cell lung cancer cells uncovers functional compensation among isoforms. *Cancer Biology & Therapy*, *16*(9), 1341–1352.

Wellman, T. L., Eckenstein, M., Wong, C., Rincon, M., Ashikaga, T., Mount, S. L., … Lounsbury, K. M. (2014). Threonyl-tRNA synthetase overexpression correlates with angiogenic markers and progression of human ovarian cancer. *BMC Cancer*, *14*(1), 1–9.

White, E., Mehnert, J. M., & Chan, C. S. (2015). Autophagy, Metabolism, and Cancer. *Clin*

Cancer Res, *21*(22), 5037–5046.

Wilkinson, B., Gregory, M. A., Moss, S. J., Carletti, I., Sheridan, R. M., Kaja, A., … Mendez, C. (2006). Separation of anti-angiogenic and cytotoxic activities of borrelidin by modification at the C17 side chain. *Bioorganic & Medicinal Chemistry Letters*, *16*, 5814–5817.

Williams, T. F., Mirando, A. C., Wilkinson, B., Francklyn, C. S., & Lounsbury, K. M. (2013). Secreted Threonyl-tRNA synthetase stimulates endothelial cell migration and angiogenesis. *Scientific Reports*, *3*, 1–7.

Xu, G., Wang, X., Yu, H., Wang, C., Liu, Y., Zhao, R., & Zhang, G. (2019). Beclin 1, LC3, and p62 expression in paraquat-induced pulmonary fibrosis. *Human & Experimental Toxicology*, *20*(10), 1–9.

Yang, M., Mckay, D., Pollard, J. W., & Lewis, C. E. (2018). Diverse Functions of Macrophages in Different Tumor Microenvironments. *Cancer Research*, *78*(19), 5492–5503.